Positron annihilation study of Fe-ion irradiated reactor pressure vessel model alloys

Chen, L.; Li, Z. C.; Schut, H.; Sekimura, N.

Important note
To cite this publication, please use the final published version (if applicable).
Please check the document version above.

PAPER • OPEN ACCESS

Positron annihilation study of Fe-ion irradiated reactor pressure vessel model alloys

To cite this article: L Chen *et al* 2016 *J. Phys.: Conf. Ser.* **674** 012012

View the article online for updates and enhancements.

Related content

Recent citations

Positron annihilation study of Fe-ion irradiated reactor pressure vessel model alloys

L Chen[1,4], Z C Li[2,5], H Schut[3] and N Sekimura[4]

[1]State Key Laboratory of New Ceramics and Fine Processing, School of Materials Science and Engineering, Tsinghua University, Beijing 100084, China
[2]Key Laboratory of Advanced Materials (MOE), School of Materials Science and Engineering, Tsinghua University, Beijing 100084, China
[3]Department of Radiation Science and Technology, Delft University of Technology, Mekelweg 15, 2629 JB Delft, the Netherlands
[4]Department of Nuclear Engineering and Management, The University of Tokyo, 7-3-1 Hongo Bunkyo-ku, Tokyo 113-8656, Japan

Email: zcli@tsinghua.edu.cn

Abstract. The degradation of reactor pressure vessel steels under irradiation, which results from the hardening and embrittlement caused by a high number density of nanometer scale damage, is of increasingly crucial concern for safe nuclear power plant operation and possible reactor lifetime prolongation. In this paper, the radiation damage in model alloys with increasing chemical complexity (Fe, Fe-Cu, Fe-Cu-Si, Fe-Cu-Ni and Fe-Cu-Ni-Mn) has been studied by Positron Annihilation Doppler Broadening spectroscopy after 1.5 MeV Fe-ion implantation at room temperature or high temperature (290 ℃). It is found that the room temperature irradiation generally leads to the formation of vacancy-type defects in the Fe matrix. The high temperature irradiation exhibits an additional annealing effect for the radiation damage. Besides the Cu-rich clusters observed by the positron probe, the results show formation of vacancy-Mn complexes for implantation at low temperatures.

1. Introduction

The irradiation-induced embrittlement of nuclear reactor pressure vessel (RPV) steels is of great concern for the safety of the nuclear power plant (NPP) operation and possible lifetime prolongation since the first-generation reactors are approaching their initially designed operation lifetimes [1]. The basic task of nuclear reactor safety research is assessing the integrity of the RPV and its reliable lifetime prediction. Fundamental mechanisms associated with the embrittlement of RPV steels comprise the formation of solute clusters, matrix damage and grain boundary segregation, and have been studied in many comprehensive works [2-14]. However, there are still research issues that remain to be addressed, such as the mechanisms for the formation of vacancy-solute complexes.

The positron is a very suitable probe enabling sensitive detection of vacancy-containing damage in metals [15,16]. As anti-particle of the electron, the positron is trapped and annihilates at vacancy-type defect because at these sites the repelling Coulomb force due to the positively charged atomic nuclei is absent [17]. In addition, positrons annihilate sensitively at the solute clusters due to the difference in

---

5   To whom any correspondence should be addressed.

positron affinity of the alloying atoms in comparison with the host Fe matrix [18,19]. The positron affinities found in the literature of the key alloying elements in this study are: -3.84 eV for Fe, -4.81 eV for Cu, -4.46 eV for Ni and -3.72 eV for Mn [18].

In the present paper, the Positron Annihilation Doppler Broadening (PADB) spectroscopy experiments were conducted to characterize the radiation damage in Fe-ion irradiated RPV model alloys, including Fe, Fe-Cu, Fe-Cu-Si, Fe-Cu-Ni and Fe-Cu-Ni-Mn. The results provide information on the formation of vacancy-type defects, Cu-rich clusters and vacancy-Mn complexes.

2. Materials and irradiation conditions

Five different series of RPV model alloys (in total eight types) were fabricated in the shape of a bar with a cross section of 10×10 mm^2 with growing chemical complexity, i.e. Fe (a purity of 99.95%), Fe-Cu, Fe-Cu-Si, Fe-Cu-Ni and Fe-Cu-Ni-Mn. The chemical composition of the alloys is provided in table 1. A final heat treatment at 900 ^{o}C for 30 minutes followed by water quenching was performed to release the stresses. From the bar specimens of size $10 \times 10 \times 2$ mm^3 were prepared by wire cut electrical discharge machining. Finally the surfaces of all samples were polished to a mirror finish with metal polishing paper and diamond lapping.

Table 1. The chemical composition of the studied alloys.

Series	Concentration (wt.%)			
	Cu	Ni	Mn	Si
Fe	≤ 0.0001	≤ 0.0012	≤ 0.00025	≤ 0.0004
Fe-Cu	0.5	-	-	-
Fe-Cu-Si	0.5	-	-	0.1
	0.5	-	-	0.2
Fe-Cu-Ni	0.5	0.6	-	-
	0.5	0.8	-	-
Fe-Cu-Ni-Mn	0.5	0.6	1.4	-
	0.5	0.8	1.4	-

The eight types of specimens have been irradiated at room temperature (RT) with 1.5 MeV Fe ions at the 320 kV implantation platform at the Institute of Modern Physics, Chinese Academy of Sciences, to doses of 0.03 dpa, 0.06 dpa and 0.14 dpa (0.1 dpa corresponding to about 40 years of radiation and the theoretical end-of-life of the NPPs). In addition, five types of specimens, Fe, Fe-0.5%Cu, Fe-0.5%Cu-0.2%Si, Fe-0.5%Cu-0.8%Ni and Fe-0.5%Cu-0.8%Ni-1.4%Mn were selected to be irradiated at 290±10 ^{o}C (high temperature, denoted as "HT") to a dose of 0.14 dpa, as RPVs in service operate at about 290±30 ^{o}C. In the present paper, Fe^{10+} was used for the implantation (i.e. ion irradiation) and the implantation flux is 1.2×10^{11} cm^{-2}s^{-1}. The damage level, dpa associated with the ion irradiation was determined by SRIM. The quick Kinchin and Pease option with a displacement energy of 40 eV and a lattice binding energy of 0 was run, and then the number of displacements was calculated according to the damage energy to be most consistent with the internationally-recognized standard NRT dpa, as recommended by Stoller R E et al. [20]. Then the dose rate D in dpa/s can be calculated as follows:

$$D = \frac{F N^{id}}{\rho} \tag{1}$$

where F is the ion flux, N^{id} the number of displacements per ion and per depth and ρ the target's atom density of 8.48×10^{22} atoms/cm^3. This leads to a dose rate of 1.5×10^{-4} dpa/s (peak value) for the Fe-ion implantation in this present paper.

3. Measurement and analysis

The PADB measurements were carried out at the Delft ^{22}Na-source based Variable Energy Positron beam facility (VEP). This PADB spectroscopy provides not only information about open volume

defects but also about the chemical environment of the positron annihilation site by measuring the momentum distribution of the electron-positron annihilated pair.

The momentum of the electron-positron pair prior to annihilation produces a Doppler shift $\Delta E = \pm p_L c/2$ on the energy of the two annihilation photons [21,22]. Here p_L is the longitudinal component of the momentum along the direction of the gamma ray emission and c is the speed of light. The overall effect is observed as a Doppler broadening the 511 keV photo-peak in the annihilation gamma spectrum.

SRIM calculations show that the damage caused by the implantation of the 1.5 MeV Fe ions is below 800 nm with a maximum at a depth of about 450 nm. For the PADB experiments, the maximum positron implantation energy is 25 keV which corresponds to a positron mean implantation depth of about 900 nm, thus covering the sub-surface damage region.

The PADB spectra were currently measured with one gamma detector in order to get an overview of the irradiation damage along the entire Fe-ion implantation depth. Two Doppler parameters, S and W were extracted from each spectrum. The S parameter is the ratio of low-momentum region in the PADB spectrum to the total region, and the W parameter is the corresponding fraction of high-momentum annihilations. Besides showing S (W) data versus positron implantation depth (d), it is convenient to represent the data in S-W plots with energy (or mean implantation depth) as running parameter).

4. Results and discussion

As previously mentioned, in the present systems, the positrons are sensitively trapped at vacancy-type sites (i.e. vacancy-type defects and vacancy-solute complexes) and in nano-sized solute cluster with high (absolute value) positron affinity.
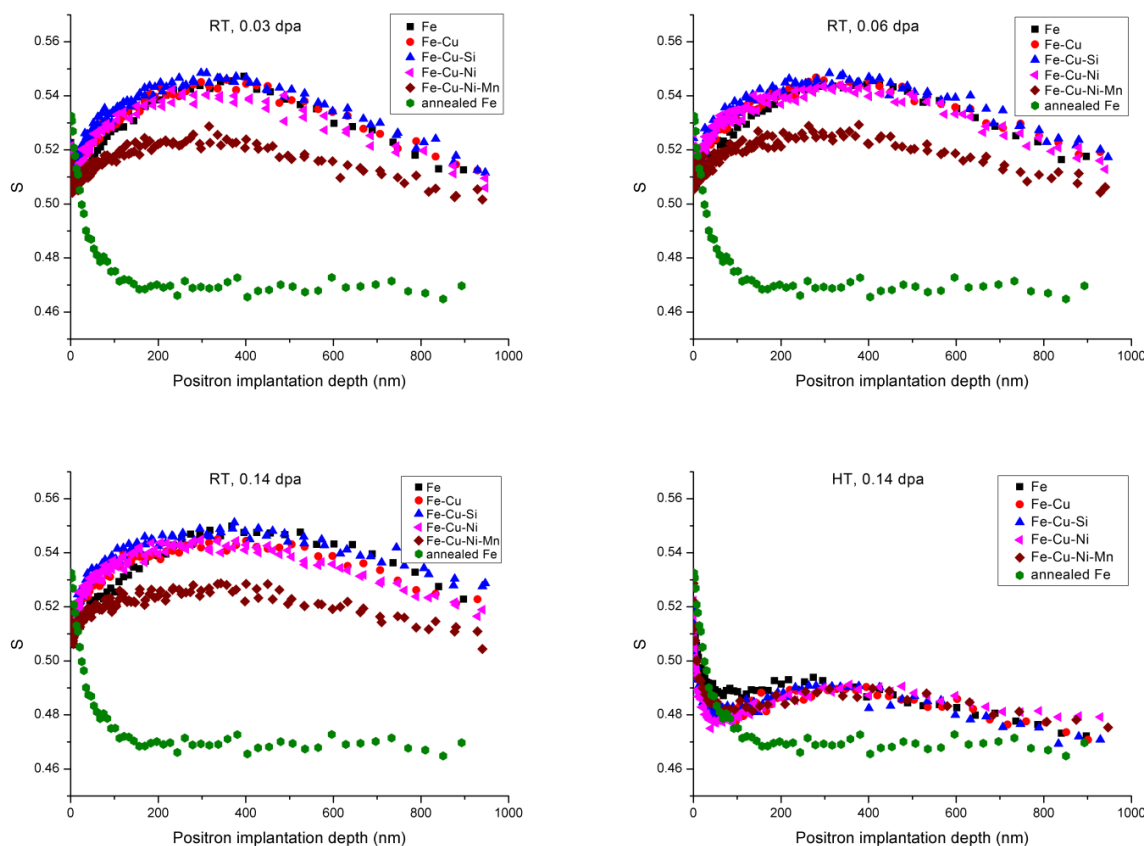

Figure 1. The S parameter as a function of positron mean implantation depth of all samples for the different implantation doses (0.03 dpa, 0.06 dpa and 0.14 dpa) at RT and for 0.14 dpa at HT.

Figure 1 shows the *S* parameter as a function of positron mean implantation depth of all samples for the different implantation doses (0.03 dpa, 0.06 dpa and 0.14 dpa) at RT and for 0.14 dpa at HT. The S curves approaching an *S* value of 0.47 are obtained for an annealed Fe sample (an extra non-irradiated Fe which is annealed after surface treatment). For all samples the behavior of the *W* parameter is roughly the inverse (high *S* - low *W*) and is therefore not shown. The data of the RT implantations show virtually no dose dependence indicating positron saturation trapping. Furthermore it can be seen that for alloys containing additional Mn the *S* parameter in the implantation range is significantly lower. For the 0.14 dpa implantation at 290 ᵒC the *S* parameter in the implantation region has reduced to a value of about 0.49 for all samples.

Figure 2 shows the *S-W* plots obtained for RT irradiated Fe, HT irradiated Fe and non-irradiated Fe as well as the annealed Fe. The arrows indicate the direction of increasing positron implantation energy or implantation depth. Starting from the surface, for the RT data the *S,W* points move into a direction of a cluster point that is also present in the non-irradiated Fe. Halfway, the points move into the direction of a line that connects the characteristic (*S,W*) cluster point for Fe with the (*S,W*) anchor point with highest *S* value. Having reached this line the data follows the line up to the highest *S* value where afterwards they follow the same line but now in the direction of the (*S,W*) cluster point for Fe. As the Fe used in this work does not contain solute elements (i.e. the content of solute elements is low enough to be neglected here), this round-trip curvature following the specific *S,W* anchor points hints at the formation of vacancy-type defect with a depth dependent defect concentration.

A closer inspection of the *S,W* data obtained at the non-irradiated Fe shows an anchor point in the near surface region (< 300 nm). This is somewhat unexpected, because in non-irradiated Fe the data should lie a straight line, as is found for the annealed Fe. The possible cause for this anchor point (which is below the defect - bulk line) is that the mechanical surface polishing has introduced near surface defects likely consisting of dislocation loops and vacancies. The figure shows that the anchor point for the HT irradiated Fe is close to the one just described for the non-irradiated Fe. The lower *S* value supposedly is caused by the additional annealing effect of the HT irradiation which effectively enables the recombination of vacancies with self-interstitial atoms [23].
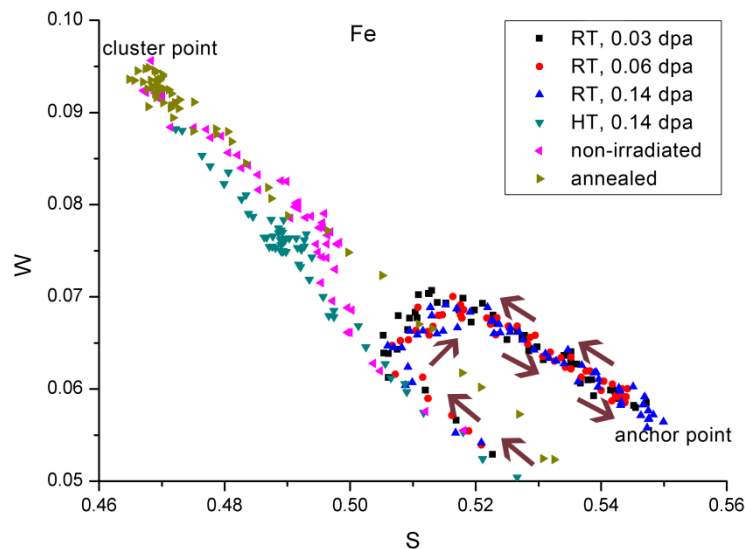

Figure 2. Results of PADB data analysis for Fe under irradiation conditions with variations in temperature and in dose as well as non-irradiated Fe and annealed Fe.

Figure 3 shows the *S-W* plots for the Fe-Cu alloy containing 0.5% of Cu. We can see that Fe-ion irradiation again leads to the round-trip curvature in the *S-W* plot for all RT irradiated Fe-0.5%Cu

alloys. It is reported that the W for elemental Cu is larger than that for elemental Fe [22] while the S parameter is only slightly lower. The effect of Cu is accordingly seen in the S-W plots in which the (S,W) anchor points belonging to the implantation region all are shifted upwards (increased W value). Also the HT data shows the round-trip behavior, but it is now located at low S, high W corner of the figure.

Compared to the RT data, the HT irradiated shows a significant lower peak value of S and its value is comparable to the one obtained for the HT irradiated Fe. The W parameter however shows a relatively larger increase. This observation can be interpreted as follows. It is well known that the Cu diffusivity depends on the vacancy concentration [12]. The annealing effect of HT irradiation in the end reduces the final vacancy concentration, but during the implantation process the available vacancies may assist the Cu diffusion leading to high number density of Cu clusters. The first effect makes the data shift into the left top corner of the graph while the latter further increases W only.
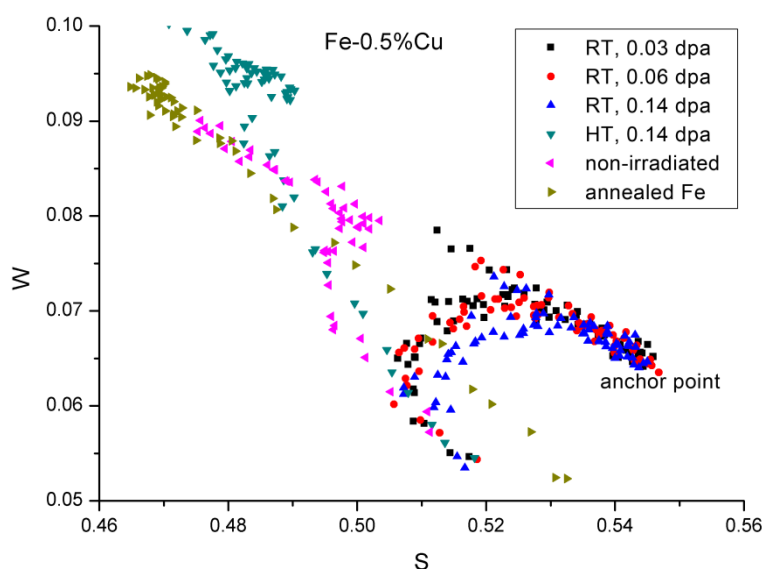

Figure 3. Results of PADB data analysis for irradiated and non-irradiated Fe-0.5%Cu alloys as well as annealed Fe.

The (S,W) points with maximum S for all RT irradiated alloys are presented in figure 4. These points are located at the end of the line which connects the (S,W) cluster point for Fe and (S,W) anchor point for the implantation defects in the S-W plots. It is clear that under Fe-ion irradiation, the Mn-containing samples (Fe-Cu-Ni-Mn) give lower values of S compared with the other samples. This is even the case when comparing the 0.14 dpa irradiated Fe-Cu-Ni-Mn with the 0.03 dpa irradiated Mn-free alloys. As mentioned before, the positron affinity of Mn is lower than that of matrix Fe. Therefore, a possible explanation is that in RT irradiated Fe-Cu-Ni-Mn alloys the vacancy-Mn complexes form efficiently, thus decreasing the content of vacancies and/or vacancy clusters. This is then unfavorable for the formation of Cu-rich clusters due to lower Cu diffusivity. In addition, the low positron affinity of Mn impedes positron trapping at the vacancy-Mn complexes. All of this leads to the decrease of S for the Mn-containing model alloys. This explanation is in agreement with the possible mechanism suggested for the effect of Mn on vacancy clusters and Cu-rich clusters: additional Mn reduces the overall vacancy diffusion, vacancy clustering, and the corresponding radiation enhanced diffusion of Cu necessary for the formation of Cu-rich clusters due to a strong interaction between Mn and individual point defects [24].
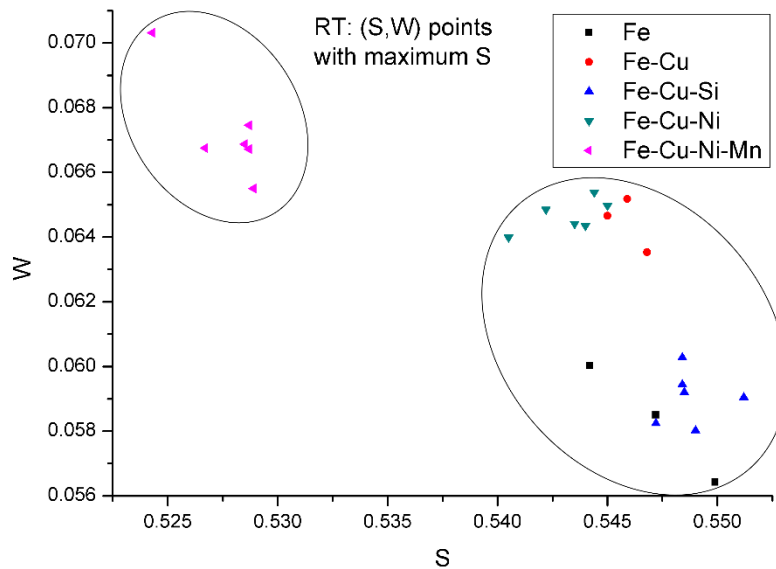
Figure 4. The (*S*,*W*) points with maximum S for all RT irradiated samples to doses of 0.03 dpa, 0.06 dpa and 0.14 dpa.

Next, the effect of Mn under HT irradiation was analyzed. Figure 5 shows the *S-W* plots for HT irradiated samples. It is observed that under HT irradiation, compared to the Mn-free alloys, the Mn-containing alloy has a lower *W* at maximum *S* for the round-trip curvature in the *S-W* plot. As reported, the *W* for elemental Mn is the lowest among those for Fe, Cu, Ni and Mn [22]. Then the low *W* observed in Fe-0.5%Cu-0.8%Ni-1.4%Mn alloy can be explained by the enrichment of Mn in Cu-rich clusters. In HT irradiated Fe-0.5%Cu-0.8%Ni-1.4%Mn alloys, there is no observation of the evidence for the formation of vacancy-Mn complexes, in terms of the lowering of the *S* value for the round-trip curvature part in the *S-W* plot. Therefore, it is reasonable to conclude that low temperature favors the formation of vacancy-Mn complexes during irradiation. Furthermore, it has been indicated that Mn-rich clusters are promoted at lower irradiation temperatures [25]. The consistency of these two microstructures with respect to the irradiation temperature supports the reported mechanism that vacancy-Mn complexes may be precursors to the formation of Mn-rich clusters [22].
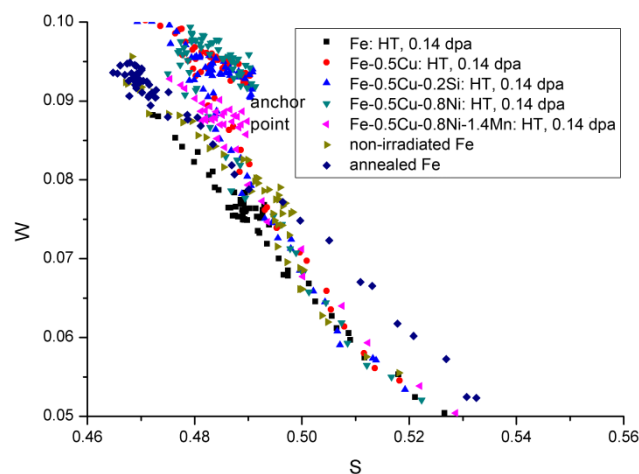

Figure 5. Results of PADB data analysis for HT irradiated Fe and Fe- alloys as well as non-irradiated Fe and annealed Fe.

5. Conclusion

The results of the PADB experiments conducted in this study are used to characterize the positron-sensitive nano features produced in the RPV model alloys (Fe, Fe-Cu, Fe-Cu-Si, Fe-Cu-Ni and Fe-Cu-Ni-Mn) subjected to 1.5 MeV Fe-ion irradiation. It is observed that vacancy-type defects are formed in RT and HT irradiated Fe and that the higher temperature leads to an additional annealing effect. The PADB measurements also show the formation of Cu-rich clusters in ion irradiated Fe-Cu alloys and HT irradiated Fe-Cu-Si, Fe-Cu-Ni and Fe-Cu-Ni-Mn alloys. The behaviors of Mn under RT irradiation and under HT irradiation are found to be different. It is shown that in Fe-Cu-Ni-Mn alloys, vacancy-Mn complexes are formed under RT irradiation, but not formed under HT irradiation. This indicates that during irradiation, low temperature favors the formation of vacancy-Mn complexes.

References

[1] Odette G R and Nanstad R K 2009 *JOM* **61** 17-23
[2] Lambrecht M and Almazouzi A 2011 *J. Phys.: Conf. Ser.* **265** 012009
[3] Styman P D, Hyde J M, Wilford K, Morley A and Smith G D W 2012 *Prog. Nucl. Energ.* **57** 86-92
[4] Toyama T, Nagai Y, Tang Z, Hasegawa M, Almazouzi A, van Walle E and Gerard R 2007 *Acta Mater.* **55** 6852-60
[5] Meslin E, Radiguet B and Loyer-Prost M 2013 *Acta Mater.* **61** 6246-54
[6] Li Z C, Abe H and Sekimura N 2007 *J. Nucl. Mater.* **362** 87-92
[7] Hernández-Mayoral M and Gómez-Briceño D 2010 *J. Nucl. Mater.* **399** 146-53
[8] Slugen V, Kögel G, Sperr P and Triftshäuser W 2002 *J. Nucl. Mater.* **302** 89-95
[9] Soisson F, Barbu A and Martin G 1996 *Acta Mater.* **44** 3789-800
[10] Stoller R E 2000 *Nucl. Eng. Des.* **195** 129-36
[11] Li Z C and Chen L 2014 *Acta Metall. Sin.* **50** 1285-93
[12] Christien F and Barbu A 2004 *J. Nucl. Mater.* **324** 90-6
[13] Schmauder S and Binkele P 2002 *Comp. Mater. Sci.* **24** 42-53
[14] Zhang Q, Li Z C, Lin C, Liu B X and Ma E 2000 *J. Appl. Phys.* **87** 4147-52
[15] Nagai Y, Takadate K, Tang Z, Ohkubo H, Sunaga H, Takizawa H and Hasegawa M 2003 *Phys. Rev.* B **67** 224202
[16] Hu Z, Li Z C, Zhou Z, Shi C Q, Schut H and Pappas K 2014 *J. Phys.: Conf. Ser.* **505** 012014
[17] Eldrup M and Singh B N 1997 *J. Nucl. Mater.* **251** 132-8
[18] Puska M J and Nieminen R M 1994 *Rev. Mod. Phys.* **66** 841-97
[19] Brauer G, Puska M J, Sob M and Korhonen T 1995 *Nucl. Eng. Des.* **158** 149-56
[20] Stoller R E, Toloczko M B, Was G S, Certain A G, Dwaraknath S and Garner F A 2013 *Nucl. Instrum. Methods Phys. Res. Sect.* B **310** 75-80
[21] Lambrecht M and Almazouzi A 2009 *J. Nucl. Mater.* **385** 334-8
[22] Glade S C, Wirth B D, Odette G R and Asoka-Kumar P 2006 *J. Nucl. Mater.* **351** 197-208
[23] Liu J, Yao H J, Sun Y M, Duan J L, Hou M D, Mo D, Wang Z G, Jin Y F, Abe H, Li Z C and Sekimura N 2006 *Nucl. Instrum. Methods Phys. Res. Sect.* B **245** 126-9
[24] Glade S C, Wirth B D, Odette G R, Asoka-Kumar P, Sterne P A and Howell R H 2005 *Philos. Mag.* **85** 629-39
[25] Lucas G E 2010 *J. Nucl. Mater.* **407** 59-69